Augmented Image Classification using Image Registration Techniques

by

Ashwini Muralidhar

A Thesis Presented in Partial Fulfillment
of the Requirements for the Degree
Master of Science

Approved November 2011 by the
Graduate Supervisory Committee:

Srikanth Saripalli, Chair
Antonia Papandreou-Suppappola
Pavan Turaga

ARIZONA STATE UNIVERSITY

December 2011

ABSTRACT

Advancements in computer vision and machine learning have added a new dimension to remote sensing applications with the aid of imagery analysis techniques. Applications such as autonomous navigation and terrain classification which make use of image classification techniques are challenging problems and research is still being carried out to find better solutions. In this thesis, a novel method is proposed which uses image registration techniques to provide better image classification. This method reduces the error rate of classification by performing image registration of the images with the previously obtained images before performing classification. The motivation behind this is the fact that images that are obtained in the same region which need to be classified will not differ significantly in characteristics. Hence, registration will provide an image that matches closer to the previously obtained image, thus providing better classification. To illustrate that the proposed method works, naïve Bayes and iterative closest point (ICP) algorithms are used for the image classification and registration stages respectively. This implementation was tested extensively in simulation using synthetic images and using a real life data set called the Defense Advanced Research Project Agency (DARPA) Learning Applied to Ground Robots (LAGR) dataset. The results show that the ICP algorithm does help in better classification with Naïve Bayes by reducing the error rate by an average of about 10% in the synthetic data and by about 7% on the actual datasets used.

DEDICATION

To my parents, grandparents and my entire family, who, have always believed in me.

ACKNOWLEDGMENTS

I would firstly like to thank Dr.Srikanth Saripalli for providing me an opportunity to work under him and for providing valuable motivation, suggestions and guidance throughout my research. I would also like to thank Dr.Antonia Papandreou-Suppappola and Dr.Pavan Turaga for kindly agreeing to serve on my dissertation committee. I am also thankful to my family and friends who have showered me with support and encouragement in times of need during this journey.

TABLE OF CONTENTS

Page

LIST OF TABLES

Table Page

LIST OF FIGURES

Figure Page

Chapter 1

INTRODUCTION

1.1 Motivation

Imagery forms one of the most important forms of remote sensing. Photogrammetry techniques, originated in 1849, were amongst the first to use photographs for preparing topography maps [1]. From there, remote sensing imagery has come a long way including infra-red imagery, multispectral imagery and satellite imagery [1]. Image classifiers are used in remote sensing for autonomous navigation, agriculture, mining and environmental research. Image registration techniques have also been used independently in remote sensing for fusing images obtained from multiple sensors [2] or to fuse images captured at different resolutions [3]. In this dissertation, an approach based on combining the method of image classification and image registration in order to help remote sensing applications, particularly autonomous navigation and terrain classification, is proposed.

Autonomous navigation – dealing with the navigation of vehicles without human supervision and terrain classification – dealing with the classification of terrains for purposes such as agricultural or navigational; are amongst the various applications of remote sensing data. Image processing and computer vision have come to play a very important role in these areas. Image classifiers are used to process images obtained by the unmanned vehicle on a terrain and help the vehicle make decisions on how to traverse on a path.

In remote sensing applications involving image classifiers, images can be obtained in the form of a video on the chosen path or images can be obtained from the same location at different time instants. In the case of videos, the

images obtained are very similar to the ones previously obtained, with slight changes. The images obtained at a single location might be oriented slightly differently from the previous set of images. Hence, with the similarity and slight changes in the images, it is expected that registering an image prior to classifying it would provide much better classification results.

In this dissertation, simple classification and registration algorithms are used to show that registration prior to classification provides lesser error rate. The objective is to prove that the proposed method works for very simple algorithms which are low in complexity in terms of the features and parameters required. Once it is shown that it works for simple algorithms, the method can surely be extended to more complex ones. Naïve Bayes classifier [38] is used for the image classification part and iterative closest point algorithm [21] is used for the image registration part. The emphasis is not on choosing a classification or registration method that provides the best results individually but more so to prove that on combining the two of them there is a considerable improvement in performance.

The performance of different image classifiers varies according to the features selected, the type of dataset used, the number of images used for training and so on. The performance might deteriorate in challenging conditions and in such situations the proposed method would be most beneficial in boosting the performance. In time consuming algorithms, input conditions can be relaxed and this method can be used to obtain similar or better performance, but at a much faster rate.

1.2 Related Work

The navigation of an unmanned rover largely depends on the type of terrain it is on. Terrains can be roughly classified as swampy, marshy, urban, wood and so on [4]. Imagery based terrain classification has found vast importance due to the prior judgment these algorithms provide [5]. This information can be used in order to determine if the terrain is smooth or rough, hard or slippery and in turn determine if the path is traversable or not. The analysis determines the obstacles in the immediate path of the rover and guides it around the obstacle onto a traversable path.

The main factors to be considered for such classification are the performance of an algorithm for the given task and the features chosen for classification. The algorithm can be either a supervised or unsupervised classifier. Supervised classification uses labeled images in order to aid classification, whereas unsupervised learning depends on the features present in the data. Simple supervised classifiers are Naïve Bayes classifier [38], k-nearest neighbor classifiers [41] whereas k-means [42] and fuzzy c means clustering [43] are the simple unsupervised classifiers available. More complex classifiers such a support vector machines [44] for supervised and principal component analysis [45] for unsupervised are also available for more refined results. The advantage of using supervised classifiers is that the prediction accuracy is higher for this case [6]. The cost associated with the labeling in supervised classifiers can act as a disadvantage in cases where the characteristics change with time. In such cases, using unsupervised learning is advisable. Supervised learning is used in this research since the dataset that is used is an already labeled dataset and hence that can be used advantageously to obtain better performance.

Related work using Naïve Bayes Classifier

As mentioned earlier, the Naïve Bayes classifier is chosen in this research for its simplicity. Naive Bayes classifiers have been used in various remote sensing scenarios. [7] have successfully used Naïve Bayes for autonomous terrain classification for robot navigation. Their analysis on 4 different datasets using texture, color or a combination of both as features shows results on par with many offline classifiers. [8] provides a method for omnidirectional image segmentation for robot navigation. The method provided results for prolonged periods of time when tested on robots. [9] uses Naïve Bayes in conjunction with support vector machines in order to control the velocity of motion of the rover. Apart from these, Naïve Bayes is also used in various other remote sensing applications such as soil erosion assessment [10], annotation of planetary surfaces [11] and so on.

Related work using Iterative Closest Point algorithm

Iterative closest point algorithm is a simple image registration algorithm and has been independently used in various remote sensing applications including terrain classification. [12] shows that ICP can reduce the dependency of global positioning systems in position estimation for unmanned aerial vehicles. [13] uses ICP to match two different images taken at the same scene using different sensors under different operating conditions. [14] proposes a method to match seabed terrains which allows for underwater vehicle navigation and it makes use of probabilistic data association filtering and iterative closest contour point methods. [15] also helps in underwater navigation by using a combination of ICP algorithm and geomagnetic reference to perform location positioning.

Related work using image classification and registration techniques

This section surveys existing methodologies and applications that make use of both image classification and image registration techniques. On exploring the existing literature in the field of remote sensing, work that involves image classification to aid in better registration were found. [16] works on finding a long term registration between under water images. Since registration is to be carried out with images obtained in time intervals of weeks or months together, spatial and temporal variations on the sand-bed are common problems encountered. [16] aims to using image segmentation and image classification to aid better registration. Features obtained from Gabor wavelets were used to perform linear discriminant analysis followed by a nearest neighbor classifier. This method gave results for coarse registration. [17] also aims at improving registration of images obtained from multiple sensors by using image classification. The scale invariant feature transform (SIFT) that are generally used for image registration performs poorly in case of registering images from multiple sensors. In this paper, a new method is proposed which uses a combination of SIFT descriptors and maximum likelihood classification for better performance.

Literature in the medical field suggests that image registration to obtain better classification has been used in certain cases. Classification of tumors as cancerous or benign is a very important task in oncology. Tumors undergo slight alterations during an ultrasound testing and hence [18] suggests a method where the post and pre ultrasound images are registered and then classified for testing. The registration uses mutual information between images whereas classification uses support vector machines.

Multiples or multi-color fluorescence in situ hybridization(M-FISH) image classification technique, which views specimens with multiple labels in different color channels, is used for cancer diagnosis. A common problem faced in M-FISH imaging is misalignment amongst pixels. [19] suggests a method for multi-resolution registration to solve this problem. [19] uses Levenberg-Marquardt algorithm to perform registration following which a Bayesian classifier is used for pixel by pixel classification. [20] also works on similar premises in order to monitor tumors and tissues better by image registration and then image classification. The paper suggests finite element modeling and surface projection alignment of required regions for registration.

It is noticed that although medicinal imaging does incorporate registration techniques to aid classification, it must be noted that in this case it is registering images of the same object taken at the same position with some time interval while, in this research, the images are from a moving camera. And in remote sensing applications, image classification is used to aid registration, thus making the method proposed in this research a novel method.

Chapter 2

DESCRIPTION OF ALGORITHMS

2.1 Naïve Bayes Classifier

The naïve Bayes classifier is a simple yet competitive and effective probabilistic classifier that makes use of Bayes theorem [39]. Bayes theorem can be explained as follows:

$$p\left(\frac{Y_i}{X}\right) \propto \prod_{k=1}^{n} p\left(\frac{x_k}{Y_i}\right) * p(Y_i) \tag{2.1}$$

where X and Y are random variables, $p\left(\frac{Y_i}{X}\right)$ is the probability of Y belonging to class i given x and $p\left(\frac{x}{Y_i}\right)$ is the probability of x occurring given it belongs to class Y_i and p(Y) is the probability of Y.

This can also expressed as shown below:

$$posterior \propto prior \times likelihood \tag{2.2}$$

Naïve Bayes assumes class conditional independence and is a simple classification algorithm. But the algorithm has proven to produce really good results on larger datasets. The advantages of using naïve Bayes is that is can be trained and tested quickly and it works well on real life data.

Variants to naïve Bayes classifier to improve performance use approaches that rely on finding correlations amongst the features, which hence reduces the strong assumption of independence that naïve Bayes is based on [39]. Some such approaches are tree-augmented naïve Bayesian (TAN) network proposed in [39] and selected naïve Bayesian classifier which uses a wrapper-based feature selection [40]

In this research, naïve Bayes classifier is implemented in MATLAB using the inbuilt naïve Bayes classifier in the statistics toolbox.

Described below is an example that shows the working of naïve Bayes. Figure 2.1 is chosen as the training image whereas Figure 2.2 is chosen as the test image. Both the images are chosen from the dataset DS3A. In order to train the naïve Bayes classifier, the manual labels provided for the training image are used and the corresponding manual labels provided for the test image are used to validate the results obtained from the prediction of the classifier.

Figure 2.1: Training image from the DS3A dataset to demonstrate Naïve Bayes algorithm

Figure 2.2: Test image from the DS3A dataset to demonstrate Naïve Bayes algorithm

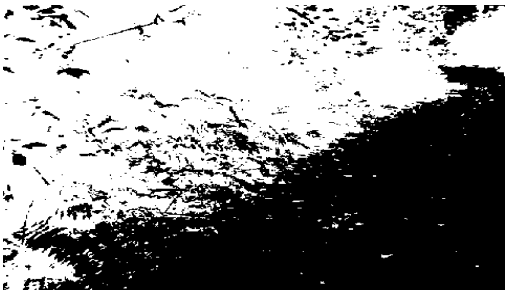

Figure 2.3: Labeled image containing predicted labels using Naïve Bayes algorithm for the test image in Figure 2.2 where black represents traversable path and white represents non-traversable path

On using the classifier, the classification rate was found to be 86.72% and figure 2.3 shows the predicted labels for figure 2.2

2.2 Iterative Closest Point Algorithm

The iterative closest point algorithm is one of the algorithms used for registering two clouds of data points. It was introduced independently by [21] and [22].

Consider data clouds X and P containing N_x and N_p points respectively. The 2 data clouds need to be registered. The iterative closest point uses the Euclidean distance metric to calculate the minimum distance between a point p in P and the data cloud X as follows

$$d(p,X) = \min_{x \in X} \|x - p\| \qquad (2.3)$$

On denoting the closest point in X to point p in P as y, we get a cloud of closest points Y which can be represented as seen below

$$Y = C(P,X) \qquad (2.4)$$

where C is the closest point operator.

The least squares registration is computed on Y with respect to P as follows in [21]

$$(q,d) = Q(P,Y) \qquad (2.5)$$

where Q is the least squares quaternion operation.[21] uses the quaternion operation whereas other forms such as singular value decomposition approach can also be used.

The mean square objective function described below is minimized to form Q, the quaternion operator

$$f(q) = \frac{1}{N_p} \sum_{i=1}^{N_p} || \vec{x_i} - R(q_r) p_i - q_t || \quad (2.6)$$

where q_r and q_t are the rotation and translation vectors.

The algorithm iterates as follows until convergence is met

- Compute the closest points for all points in the first data cloud corresponding to the second data cloud using Euclidean distance
- Compute the registration data cloud and apply the same
- Iterate until the present tolerance is greater than the change in mean square error between the points p and y

This ICP algorithm gives efficient registration and always converges monotonically. It is independent of shape of the object and also does not need any pre-processing of the data points. But the disadvantages of this algorithm are that it is susceptible to outliers and convergence might prefer local minima as opposed to global minima in certain cases.

The ICP algorithm has been improved since it has been first introduced with certain variations. High-speed variants of ICP algorithm are necessary in computer vision applications in order to obtain real time results. [32] is a high-speed variant in which selection of points is done using hierarchical and logarithmic points are selected for motion tracking. [33] combines tree search and nearest neighbor search to obtain ICP performance that is about 27 times faster than usual and [34] use pre computed voxel closest neighbors In a particular biometrics applications context to obtain faster ICP.

The ICP code used here is from [35] and this code accepts 2 mxn sized images as inputs. The code also allows flexibility in choosing the number of iterations and pyramid levels. The motion model can also be chosen as per user

preference. Translation, affine, rigid and projective models are available. A binary mask specifying out of segment and in segment values can be given as input as well, along with the choice of choosing between ordinary or robust alignment. The function outputs the image that is the registered image.

The following figures give an example of the working of the registration algorithm. Figure 2.4 is a sample image (image 1) created and figure 2.5 is image 1 rotated by 5 degrees. Figure 2.6 demonstrates the output of the ICP algorithm.

Figure 2.4: Sample image 1 to show working of ICP algorithm

Figure 2.5: Sample image 2 generated by rotating image 1 by 5 degrees

Figure 2.6: Resultant image of the ICP registration algorithm with the inputs as image 1 and image 2

Chapter 3

DESCRIPTION OF DATASETS

In this study, the hand-labeled DARPA (Defense Advanced Research Project Agency) LAGR (Learning Applied to Ground Robots) datasets [36] are used. The datasets consists of data collected from 3 different types of terrain in different lighting scenarios. In total, there are 6 datasets with 100 images in each dataset for training and testing purposes. Each image is hand-labeled into one of the three groups – obstacle (1), ground plane (0) or unknown (2), with an average of 20% of pixels labeled as unknown in every image.

A brief description of the datasets is provided below [37]:

Dataset DS1A

This dataset consists of 100 images captured on a very sunny day. The path consists of hay bales and trees on one side and the color of the hay bales matches with the reddish brown color of the ground. The lighting is very bright in most cases in this dataset and the trees have often cast large shadows on the ground. It is overall a tough dataset for classification due to the unsatisfactory weather conditions present.

Dataset DS1B

This dataset consists of the 100 images captured at the same place as in DS1A but under significantly differing weather conditions. The sunlight is not glaring into these images and the path and the obstacles (hay bales and trees) are distinguishable which allows for easier machine classification as compared to DS1A.

Dataset DS2A

This dataset consists of a path covered with bushes and trees on multiple locations which makes for a tough traversable path. The sky is blue and distinguishable in this dataset. The bushes and trees are largely leafless and brown and similarly colored as the ground making this dataset also a tougher one for classification purposes.

Dataset DS2B

This dataset captured on a different day as compared to DS2A is better in terms of the lighting conditions. The better lighting conditions allow for a mediocre distinction between the bushes and the ground, although at some places shadow effects nullifies the distinction.

Figure 3.1: Representative image from DS1A dataset

Figure 3.2: Representative image from DS1B dataset

Dataset DS3A

Consisting of dense green shrubs on either side of a clear brown ground path makes this dataset the easiest dataset of the ones considered. Some parts of the ground filled with green grass can appear as non-traversable and might be misclassified as obstacle in this dataset.

Dataset DS3B

The same scenario as in DS3A but captured on a less sunny day make up dataset DS3B. This dataset appears darker but a clear distinction between green and brown areas are possible, making this also an easy dataset. Again, the grassier parts of the grounds are at the risk of miscalculation due to the similar

Figure 3.3: Representative image from DS2A dataset

Figure 3.4: Representative image from DS2B dataset

Figure 3.5: Representative image from DS3A dataset

Figure 3.6: Representative image from DS3B dataset

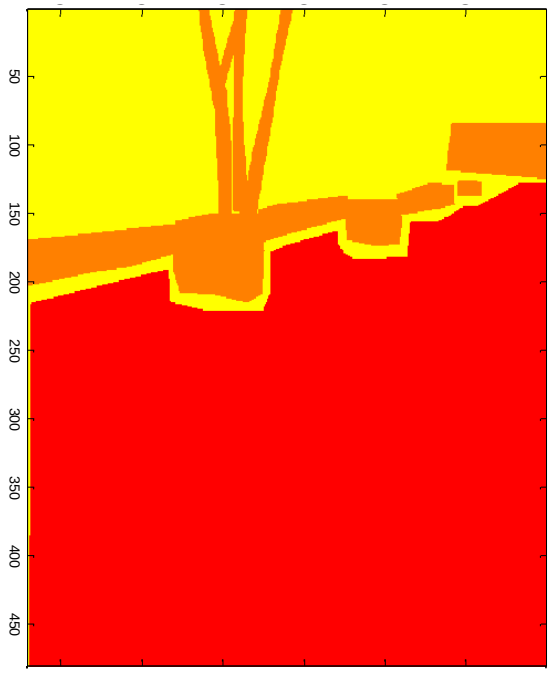

Figure 3.7: Representative image of the manual labels for an image from DS1B dataset where red represents ground plane, orange represents obstacle and yellow represents unknown

coloring of the shrubs.

From the description of the datasets, it can be seen that the dataset provides the required diversity needed for training and testing owing to the significantly different scenarios captured at different light conditions. Hence the DARPA LAGR dataset is an interesting dataset to work with.

Chapter 4

RESULTS FROM CLASSIFICATION

In order to determine the performance of naïve Bayes classifier on the DARPA LAGR dataset, various tests were conducted by varying the training and test data. The training data along with the manual labels provided are fed to the naïve Bayes classifier. Then a prediction matrix is obtained for the train data fed into the naïve Bayes model. This prediction matrix is compared to the manual labels available for the test data and compared. The error rate is computed after comparison.

The features used for training is a weighted combination of the RGB components. The optimal weights were chosen by running the classifier for random weights for the RGB components 30 times and choosing the weights that allowed for the least error rate. The optimal weights are given below in Table 4.1

Table 4.1: Weights for RGB values

Dataset	R wt	G wt	B wt
DS1A	0.5472	0.3222	0.1306
DS1B	0.5185	0.1583	0.3233
DS2A	0.0945	0.4155	0.4900
DS2B	0.2924	0.1924	0.5152
DS3A	0.1607	0.5457	0.2936
DS3B	0.4226	0.0785	0.4989

The weights physically represent the colors based on their prominence in the dataset. On looking at DS1A and DS1B, it is evident that reddish-brown color is most dominant and hence most weight to the red color is given to obtain least

error in classification. Also, similarly, DS3A, which is bright green in color, has the most weight for green color. DS3B which is of a darker green has tinges of purple and hence maximum weight is seen for blue color for minimum error.

In order to perform Naïve Bayes, the original image was labeled based on the weighted pixel values and then it was used to train the data. A similar labeling scheme was followed in the test phase and the results were compared with the naïve Bayes prediction. This method provided inconsistent results. Hence, the labels given with each image we used and were verified with the predicted labels with the known image labels. This provided consistent results which are described below.

Case I:

Using these optimal weights for each dataset, the training and testing data numbers are varied in each dataset. That is, the training set is varied from 10 up to 90 and correspondingly the test set is reduced from 90 to 10 for every dataset and the results are shown below in Table 4.2 and are plotted in Figure 4.1

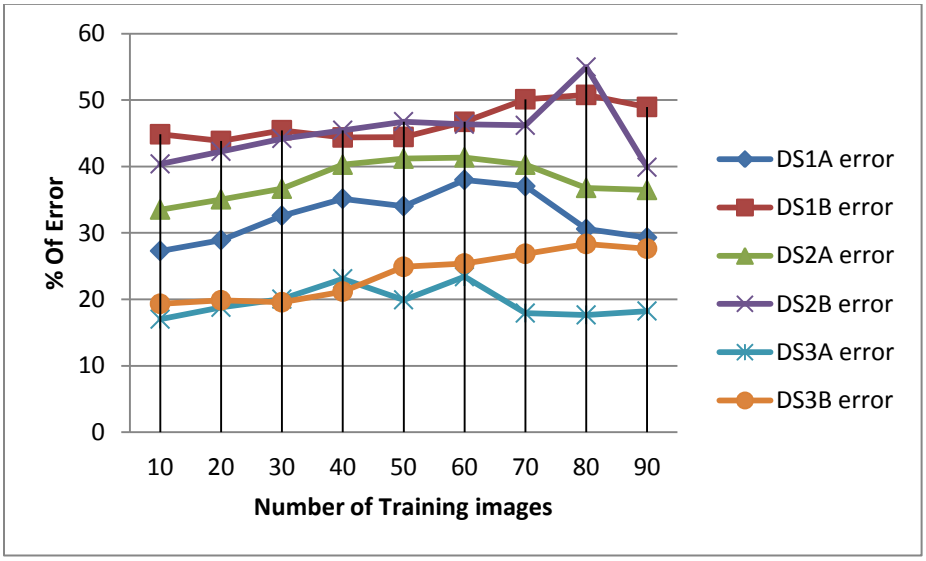

Figure 4.1: Plot of number of training images versus % of error for Case 1 for naïve Bayes Classifier

Table 4.2: Results for Case 1 for Naïve Bayes Classifier

Train	DS1A error	DS1B error	DS2A error	DS2B error	DS3A error	DS3B error
10	27.28	44.84	33.51	40.38	17.01	19.32
20	28.92	43.83	35.05	42.26	18.79	19.85
30	32.59	45.45	36.65	44.2	20.03	19.56
40	35.14	44.36	40.26	45.45	23.1	21.16
50	34.02	44.43	41.17	46.75	19.92	24.89
60	37.98	46.71	41.36	46.35	23.4	25.38
70	37.03	50.11	40.26	46.18	17.93	26.85
80	30.58	50.76	36.77	54.97	17.65	28.33
90	29.3	48.95	36.46	39.88	18.24	27.62

From the results, we can see that on training and testing with the same dataset, the error rates vary by only a small margin of about 4-5 percent. Even when the number of training images is increased, the results do not vary by a huge percentage. This is attributed to the fact that all the images in a dataset are similar to each other and hence do not provide any significant details when more training images are considered.

Also, on considering each dataset results separately, DS3A and DS3B perform best as expected. DS3A and DS3B being the easier datasets provide lower error rates of about 20% as compared to the tougher datasets DS1A, DS1B, DS2A, DS2B. These datasets have error rates varying from 35% - 45% on an

average and proves that Naïve Bayes performance is not up to the mark when we have complex datasets for analysis.

Case II:

Since the performance of Naïve Bayes is consistent on every dataset, its performance is tested on a combination of all the datasets. For this, the training set is all 100 images from one of the datasets and the testing dataset is 600 images from all the datasets put together. Such a test yielded the results shown below in Table 4.3. The plot of the same is shown in Figure 4.2

Table 4.3: Results for Case 2 for Naïve Bayes Classifier

Dataset	Error
DS1A	54.1
DS1B	46.63
DS2A	45.64
DS2B	51.97
DS3A	45.83
DS3B	41.87

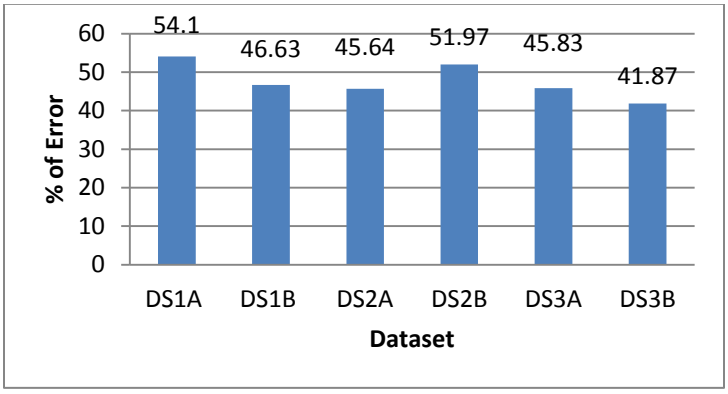

Figure 4.2: Plot of the dataset versus the percentage of error for Case 2 for naïve Bayes classifier.

From the above results we see that Naïve Bayes does not work very well when tested on different data as compared to what it was trained on. But on comparison, it shows that dataset 3 has comparatively lower error rates compared to datasets 1 and 2. Hence it shows that the performance depends on how good the training data are, which the case for datasets 3 is.

Case III:

Another way to compare was to train Naïve Bayes using images from all the datasets and test them on all 600 images. The results are provided in Table 4.4

Table 4.4: Results for Case 3 for Naïve Bayes Classifier

Training images from each dataset	Total number of training images	Testing images from each dataset	Total number of Testing images	Error Rate
10	60	100	600	36.46
20	120	100	600	36.54
20	120	20	120	37.59
10	60	10	60	36.25

In this scenario, the results are limited to 120 training images due to memory limitations in MATLAB. It is seen that in all 4 cases, the results are very close to each other. This shows that on increasing the number of training images from every dataset has no implication on the error rate. This is consistent with the results in Case I where we noticed very little difference on increasing the number of training images.

Also on comparing with Case II, we see that the error rate is considerably lesser in this Case. This proves that training with multiple datasets is better than training with the same dataset while testing on all the available data

Chapter 5

RESULTS FROM REGISTRATION

In order to prove that image classification works better after performing image registration, a simple test is employed. An image that is selected is rotated by a chosen angle and when this angle is a small number, it works as if a slightly distorted image has been obtained. Now this rotated image is tested on a Naive Bayes classifier that has been trained by the original image. Also, the two images are registered using iterative closest point algorithm and the registered image is also tested on the Naive Bayes classifier. The percentage of error obtained on classification is compared in both the cases.

In this test, the chosen image is rotated from an angle of 0 to 90 degrees and results of classification before and after registration are obtained in all the cases. The test is run on the DS1A, DS1B, DS2A, DS2B, DS3A and DS3B datasets and can be seen as shown in Figures 5.1, 5.2, 5.3, 5.4, 5.5, 5.6, respectively.

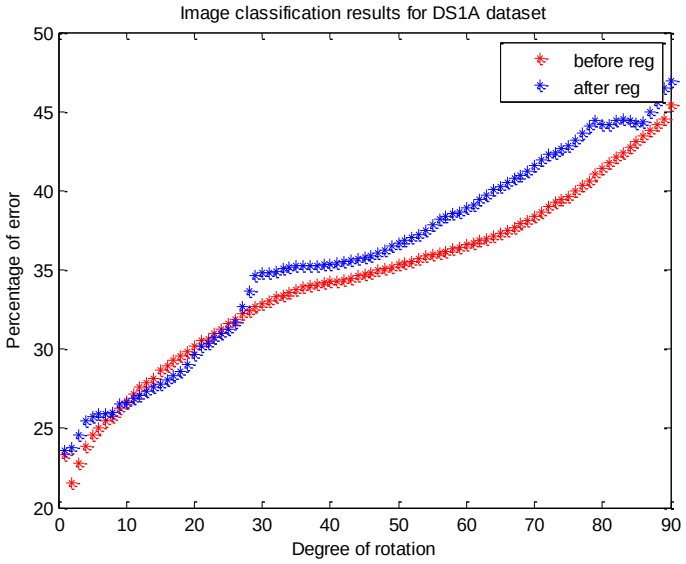

Figure 5.1: Results of image classification after registration for DS1A dataset after rotating the image from 0 to 90 degrees

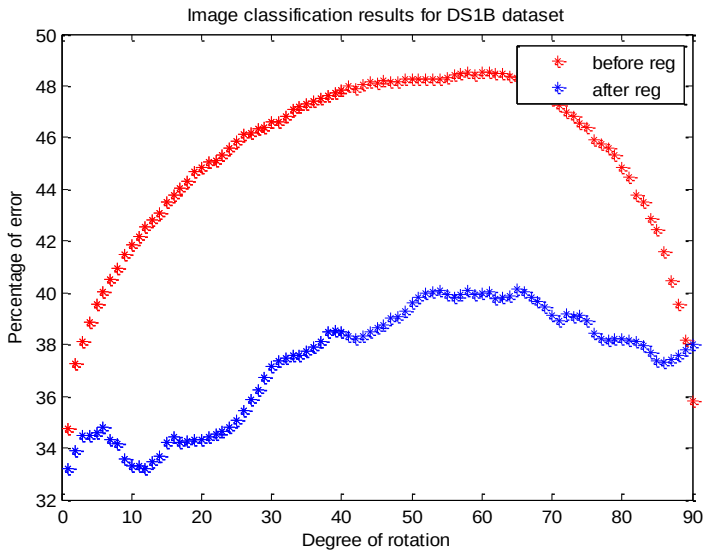

Figure 5.2: Results of image classification after registration for DS1B dataset after rotating the image from 0 to 90 degrees

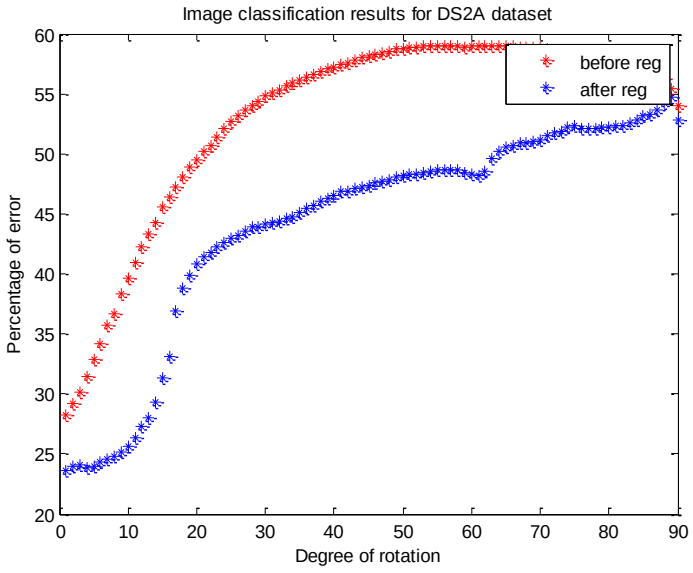

Figure 5.3: Results of image classification after registration for DS2A dataset after rotating the image from 0 to 90 degrees

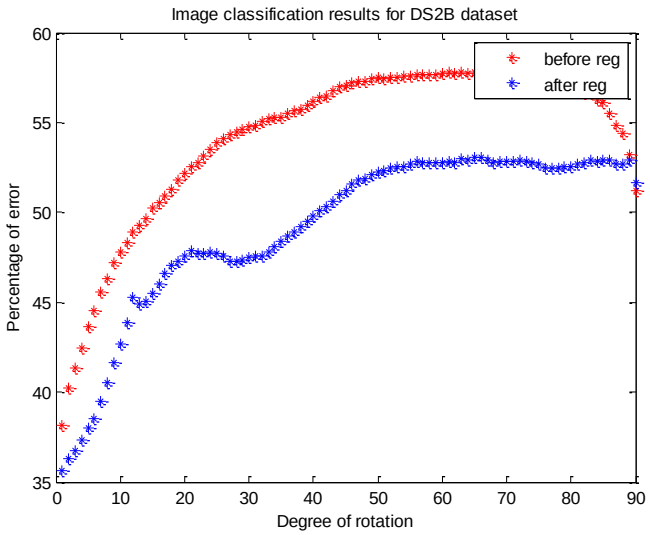

Figure 5.4: Results of image classification after registration for DS2B dataset after rotating the image from 0 to 90 degrees

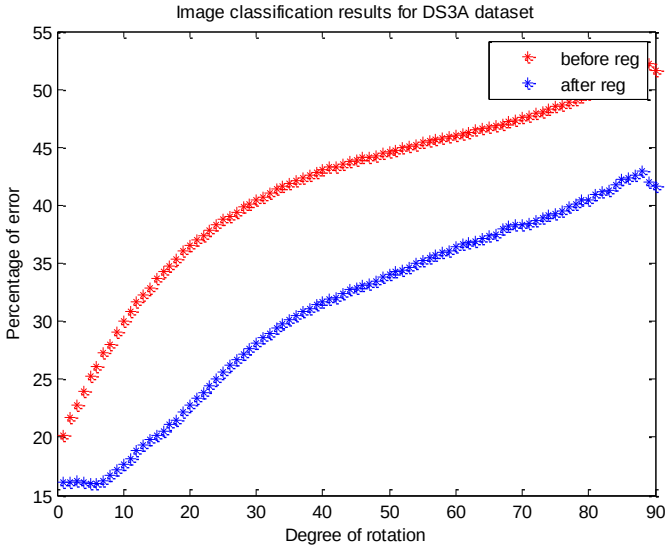

Figure 5.5: Results of image classification after registration for DS3A dataset after rotating the image from 0 to 90 degrees

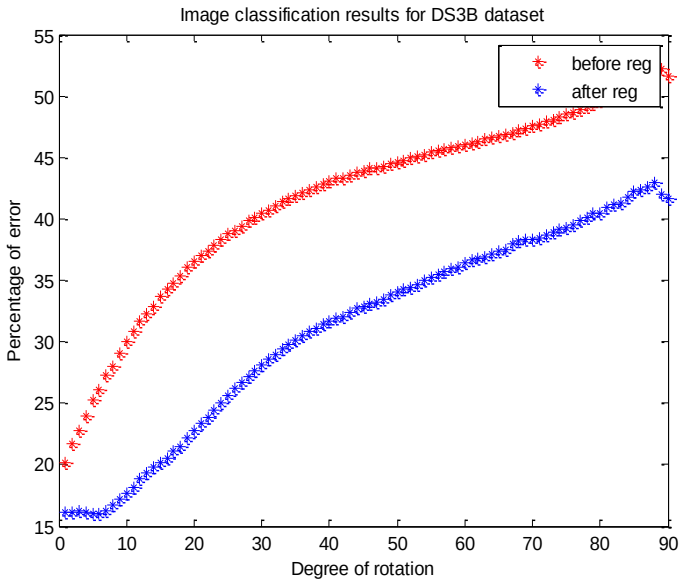

Figure 5.6: Results of image classification after registration for DS3B dataset after rotating the image from 0 to 90 degrees

From the results above, it can be seen that out of the 6 datasets the test is performed on, in 5 cases the classification error rate is lesser after registration than before. The degree of rotation is varied up to 90 degrees, which is a very large rotation for practical purposes. And quite naturally as the degree of rotation increases, the error rate increases as seen in all 6 cases. But even in such extreme rotation cases, prior registration does help in bringing down the error.

Chapter 6

RESULTS FROM REGISTRATION AND CLASSIFICATION

In this section, the results obtained by performing classification on the consecutive images present in a dataset after registering them with ICP is presented. The images in the datasets are shot at a rate of 5 frames/sec and the images for registration and classification are chosen in increments of 1, 4, 7 and 10 respectively. All the results are collected at 14 iterations and 4 pyramid levels.

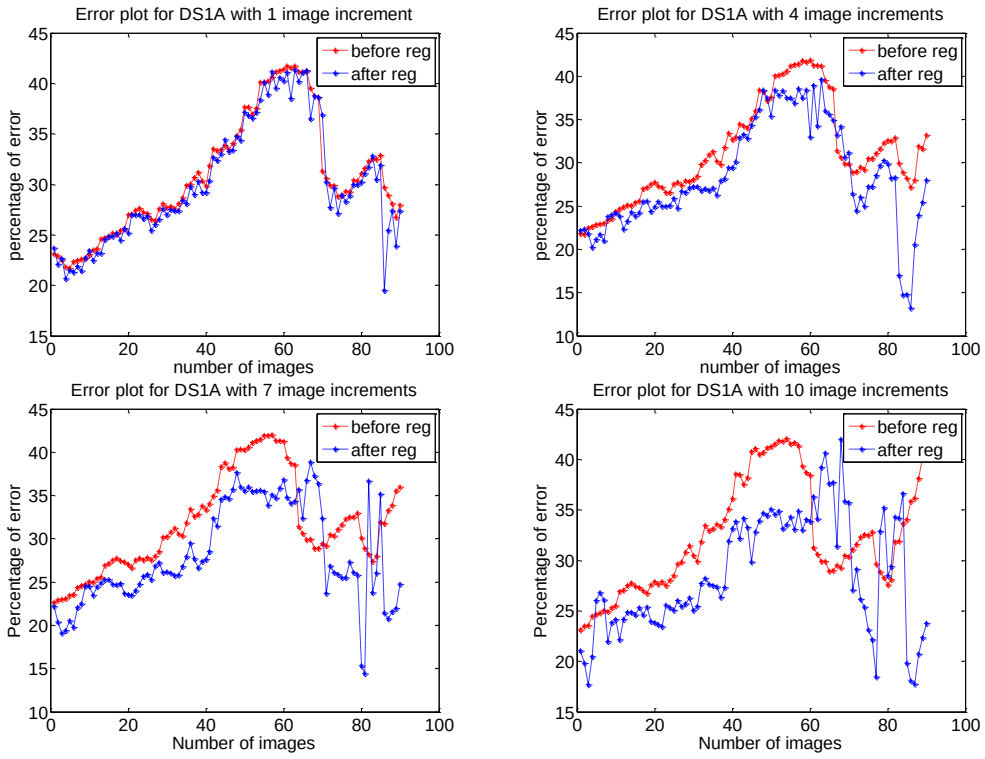

Figure 6.1: Error plot for DS1A dataset with blue representing error curve for classification after registration and red curve, before registration

In the DS1A dataset, the path is a straight path and the variations of the consecutive images of the dataset are small. On considering consecutive images, which vary by 1 or 2 degrees, since registration plays a smaller role, classification results are improved by only a couple of percent. In the case of considering

images in increments of 10, the images are rotated by about 10 degrees and hence registration helps provide good classification results. The results in Figure 6.1 show that registration helps bringing down the classification error rate by about 10 percent.

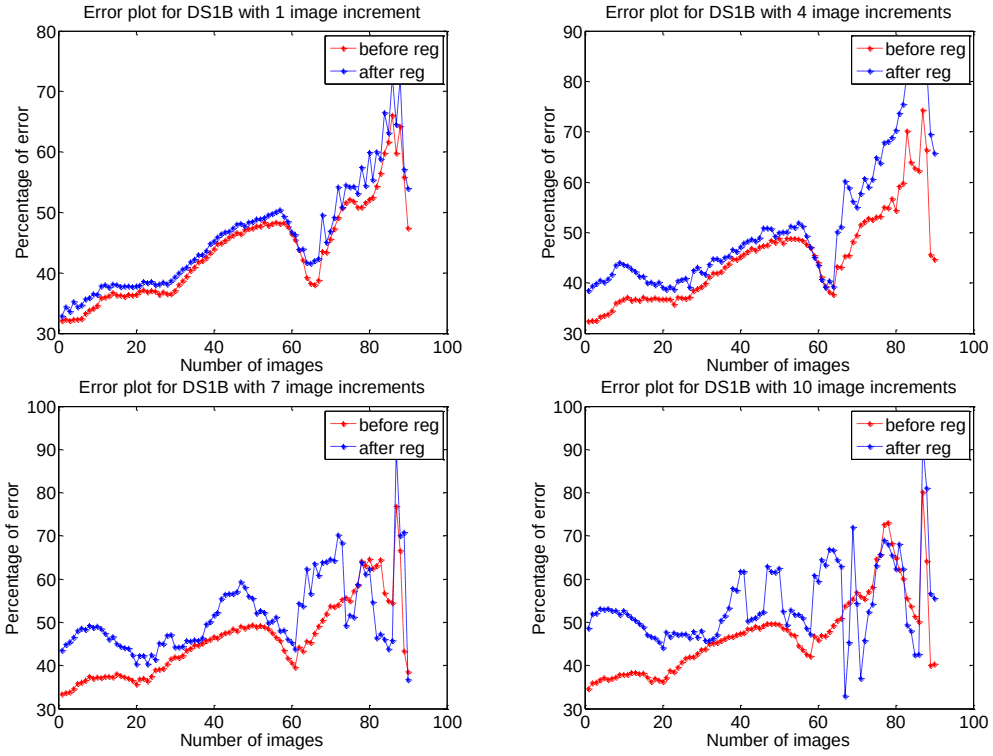

Figure 6.2: Error plot for DS1B dataset with blue representing error curve for classification after registration and red curve, before registration

Although dataset DS1B is taken on the same path as DS1A on a different day, the path traced by the rover collecting the images in the DS1B case is significantly different from the DS1A case. The rover in this case steers off the actual path after the first 20 images and gets on to hay. This creates a lot of variations in the images collected from images 30 to about 60. But beyond image 70 onwards, although the images are off the actual path, the images are quite similar. Hence the error reduction after registration works on the images

numbered 60 onwards, as can be seen in Figure 6.2.The ones before that have a lot of variations and on registration, the registered image has a lot of black regions which do not help in classification. Hence the results are not favorable. This can be illustrated below in Figure 6.3. The images numbered 40 and 50 are considered respectively and the result of the registration can be seen to produce a lot of black spaces, which while classification is misclassified as ground plane when it should actually be classified as obstacles.

(a) Image number 40 (b) Image number 50 (c)Resultant image of registration of image 50 with image 40

Figure 6.3: Registration result illustration for DS1B dataset

Dataset DS2A is a dataset that contains a lot of bushes on the path. From the results in Figure 6.4, it can be seen that registration does not help this dataset at all in bringing down the error rate of classification. This is a rapidly changing dataset, due to the movement of the rover and the shift in the position of the bushes corresponding to the rover movement. On considering images in increments of 1, 4, 7 and 10, it can be seen that the classification error rate progressively increases for the case after registration. The increase in the error is prominent in the images numbered from 40 to 70. This is because the images change most rapidly in this section and they approach the bushes here. Figure 6.5 illustrates the effect on registration results on changing the image increments for a particular image. The image considered for Figure 6.5 is image numbered 40 and column 1 shows image 40. The second column corresponds to images 41, 44,

47 and 50 respectively and the third column represents the registered image for the images in the second column. As it can be seen, as the spacing between the images considered is increased, the black regions of the registered image also increases, allowing for a lot of misclassification and hence increasing the error.

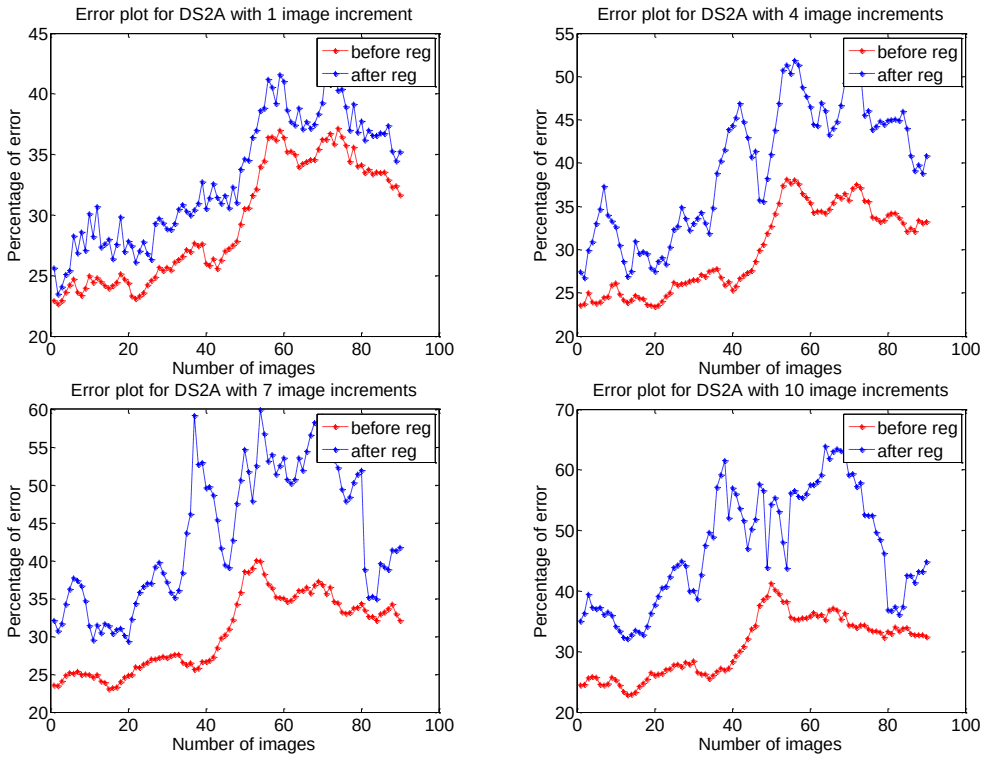

Figure 6.4: Error plot for DS2A dataset with blue representing error curve for classification after registration and red curve, before registration images

(a) Image number 40

(b) Image number 41

(c)Resultant image of registration of image 41 with image 40

(d) Image number 40

(e) Image number 44

(f)Resultant image of registration of image 44 with image 40

(g) Image number 40

(h) Image number 47

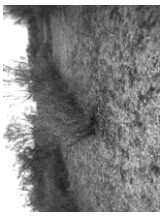

(i)Resultant image of registration of image 47 with image 40

(j) Image number 40

(k) Image number 50

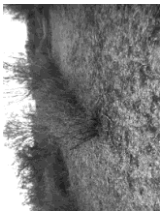

(l)Resultant image of registration of image 50 with image 40

Figure 6.5: Registration result illustration for DS2A dataset

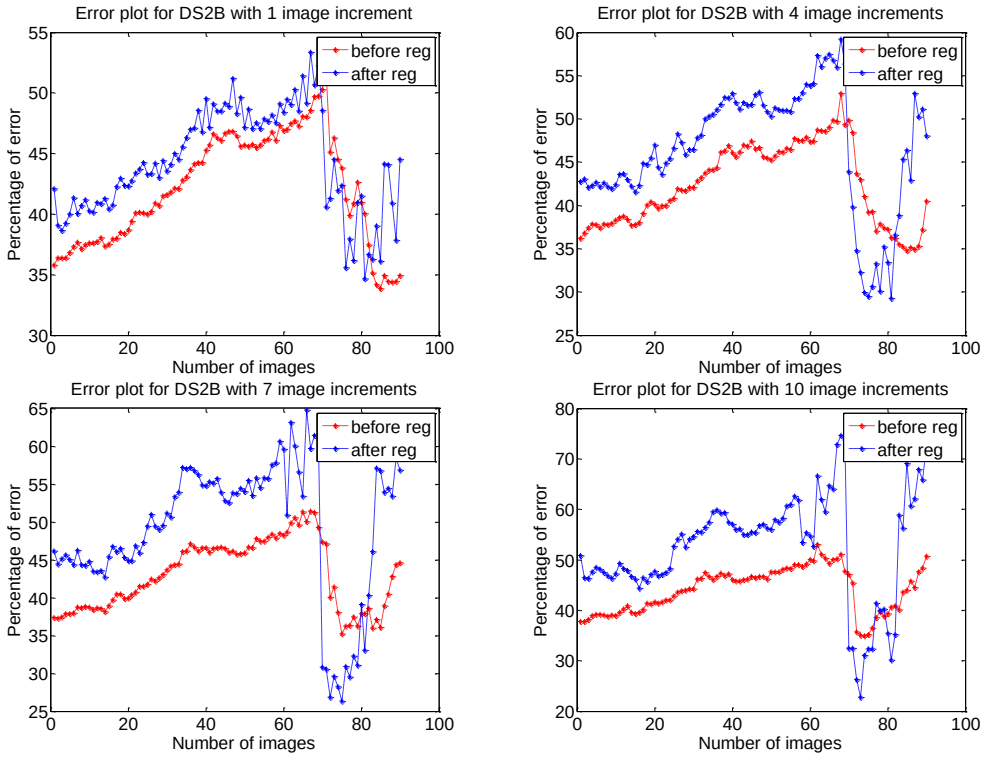

Figure 6.6: Error plot for DS2B dataset with blue representing error curve for classification after registration and red curve, before registration

Dataset DS2B is very similar in nature to DS2A. Hence, the error plot as seen in Figure 6.6 is expectedly similar, with the error rates after registration larger than before registration. But there is a section from images numbered 70 to 80, where the error rates from after registration is lesser than before registration. This is a section of the dataset that varies slowly as compared to the rest of the dataset and to dataset DS2A. Hence, Figure 6.7 illustrates the change in registration result for that section by choosing one image from the images numbered 70 to 80.Image 75, shown in column 1, is chosen and column 2 represents images 76, 79, 82 and 85 respectively. Column 3 shows the corresponding registered images for the images in column 2. Although these images shown regions in black as well, the black portions are wider along the

(a) Image number 75

(b) Image number 76

(c)Resultant image of registration of image 75 with image 76

(c) Image number 75

(e) Image number 79

(f)Resultant image of registration of image 75 with image 79

(g) Image number 75

(h) Image number 82

(i)Resultant image of registration of image 75 with image 82

(j) Image number 75

(k) Image number 85

(l)Resultant image of registration of image 75 with image 85

Figure 6.7: Registration result illustration for DS2B dataset

sides of the path, thus, not allowing for much miscalculation. Hence that section of the dataset provides lesser error compared to the rest of the dataset.

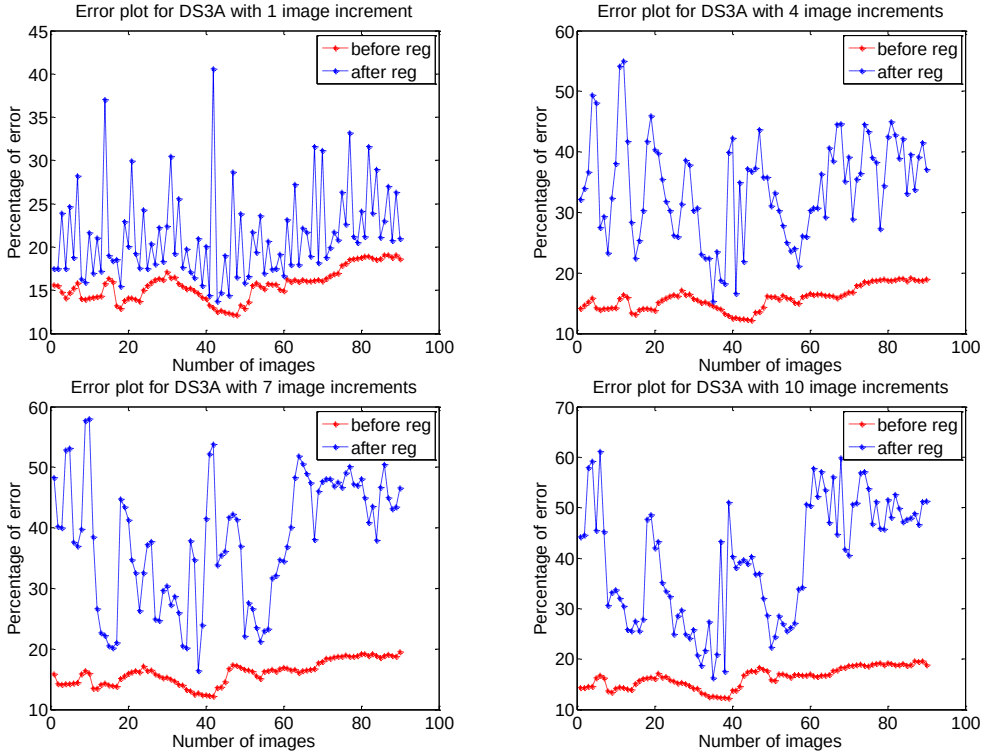

Figure 6.8: Error plot for DS3A dataset with blue representing error curve for classification after registration and red curve, before registration

Datasets DS3A and DS3B show the worst performance for image classification after registration, as shown in Figure 6.8 and Figure 6.9. This is because the DS3A dataset is along a curved path, such that each image is significantly different from the previous images and so, registration does not play a very important role as the images are not that similar. The path is surrounded by lush greenery on both sides of the curving path. Since the path is curving, registration of the image results in a lot of black spaces around the border of the image. And since 3 borders of the image consists of obstacles, which are

misclassified due to the black portions, the error rates for classification are much higher after registration.

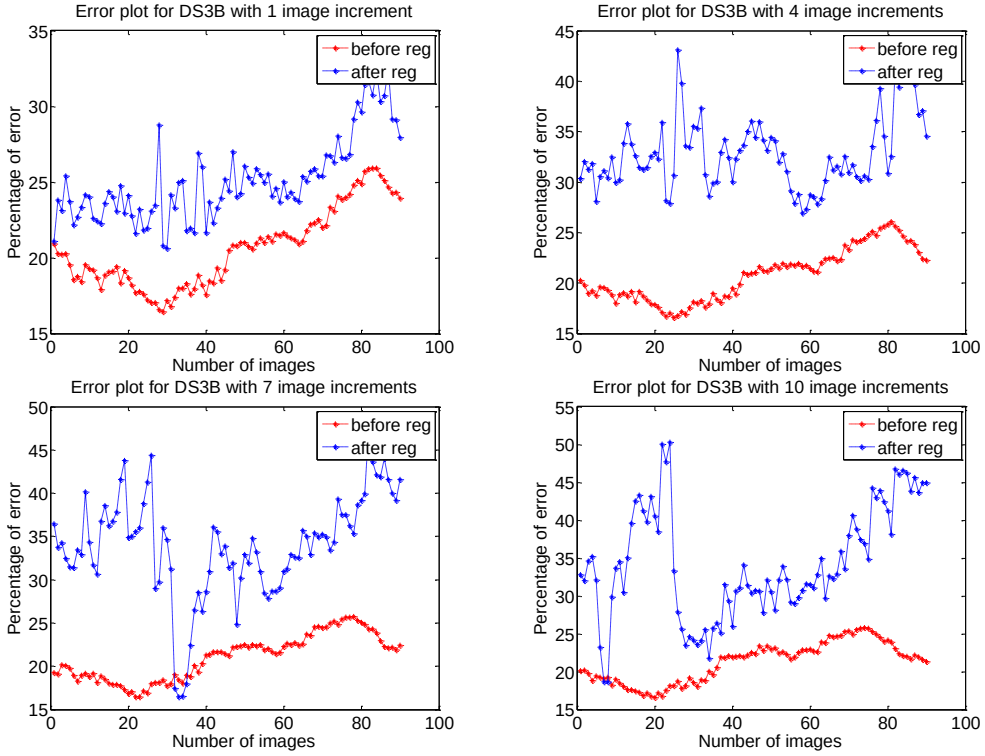

Figure 6.9: Error plot for DS3B dataset with blue representing error curve for classification after registration and red curve, before registration

Chapter 7

CONCLUSIONS

From the results presented in chapter 5, it is seen that the proposed method works well for a majority of the synthetic datasets and provides error rates of about 10% lesser on performing registration before classification. The results in chapter 6 show that for real datasets, the performance was not as expected. The error rate for classification after registration is about 7 to 8% lesser in the case of DS1A. But this is not the case with the remaining datasets. On studying the results from all the datasets, it is concluded that the performance is dependent on a lot of factors such as how well the rover traverses in a straight line on the path, if the path itself is curved or straight and the location of the obstacles. The main factor that detriments performance is that the registered image has a lot of black portions that allow for misclassification in most of the cases. In order to get better results, after registration of the image, the image must be cropped along the corners to get rid of the unwanted black portion that detriments performance. Further work can include cropping the image after registration to test the performance, and also to study other features and parameters used for registration and classification and changing them to study the effect on the performance. The advantage of cropping the registered image is that it would help in speeding up the classification since the classification is done on an image of smaller dimensions. Future work can also include testing the performance using a combination of other algorithms for classification and registration which rely on a more sophisticated set of features. Future work can also try to incorporate a method to propagate the labels in the classification for quicker and better results. The method proposed aims at augmenting image

classification techniques with image registration and on performing a more detailed study of this technique will help in providing a more sophisticated method for better classification.

REFERENCES

[1] Cohen, C.J.; , "Early history of remote sensing," *Applied Imagery Pattern Recognition Workshop, 2000. Proceedings. 29th* , vol., no., pp.3-9, 2000

[2] Hasan, M.; Xiuping Jia; Robles-Kelly, A.; Zhou, J.; Pickering, M.R.; , "Multi-spectral remote sensing image registration via spatial relationship analysis on sift keypoints," *Geoscience and Remote Sensing Symposium (IGARSS), 2010 IEEE International* , vol., no., pp.1011-1014, 25-30 July 2010

[3] Wen Hong-yan; Gao Jing-tao; , "Multi-Resolution Remote Sensing Image Registration Based on Tensor Voting," *Computer Network and Multimedia Technology, 2009. CNMT 2009. International Symposium on* , vol., no., pp.1-4, 18-20 Jan. 2009

[4]Weszka, Joan S.; Dyer, Charles R.; Rosenfeld, Azriel; , "A Comparative Study of Texture Measures for Terrain Classification," *Systems, Man and Cybernetics, IEEE Transactions on* , vol.SMC-6, no.4, pp.269-285, April 1976

[5] Chetan, J.; Krishna, M.; Jawahar, C.V.; , "Fast and Spatially-Smooth Terrain Classification Using Monocular Camera," *Pattern Recognition (ICPR), 2010 20th International Conference on* , vol., no., pp.4060-4063, 23-26 Aug. 2010

[6] Sapkal, S.D.; Kakarwal, S.N.; Revankar, P.S.; , "Analysis of Classification by Supervised and Unsupervised Learning," *Conference on Computational Intelligence and Multimedia Applications, 2007. International Conference on* , vol.1, no., pp.280-284, 13-15 Dec. 2007

[7] Happold, M.; Ollis, M.; , "Autonomous Learning of Terrain Classification within Imagery for Robot Navigation," *Systems, Man and Cybernetics, 2006. SMC '06. IEEE International Conference on* , vol.1, no., pp.260-266, 8-11 Oct. 2006

[8] Posada, L.F.; Narayanan, K.K.; Hoffmann, F.; Bertram, T.; , "Floor segmentation of omnidirectional images for mobile robot visual navigation," *Intelligent Robots and Systems (IROS), 2010 IEEE/RSJ International Conference on* , vol., no., pp.804-809, 18-22 Oct. 2010

[9] Wei Mou; Kleiner, A.; , "Online learning terrain classification for adaptive velocity control," *Safety Security and Rescue Robotics (SSRR), 2010 IEEE International Workshop on* , vol., no., pp.1-7, 26-30 July 2010

[10] Lin, Weihua; Wu, Yonggang; Mao, Dianhui; , "Region Assessment of Soil Erosion Based on Naive Bayes," *Computational Intelligence and Security, 2007 International Conference on* , vol., no., pp.6-9, 15-19 Dec. 2007

[11] Ghosh, S.; Stepinski, T.F.; Vilalta, R.; , "Automatic Annotation of Planetary Surfaces With Geomorphic Labels," *Geoscience and Remote Sensing, IEEE Transactions on* , vol.48, no.1, pp.175-185, Jan. 2010

[12] Madhavan, R.; Hong, T.; Messina, E.; , "Temporal range registration for unmanned ground and aerial vehicles," *Robotics and Automation, 2004. Proceedings. ICRA '04. 2004 IEEE International Conference on* , vol.3, no., pp. 3180- 3187 Vol.3, 26 April-1 May 2004

[13] Ionescu, D.; Abdelsayed, S.; Goodenough, D.; , "A registration and matching method for remote sensing images," *Electrical and Computer Engineering, 1993. Canadian Conference on* , vol., no., pp.710-712 vol.2, 14-17 Sep 1993

[14] Jiang Fan; Wu Yi-meng; Zhang Zhen-shan; Zhan Wu; , "Combinational Seabed Terrain Matching Algorithm Basing on Probability Data Associate Filtering and Iterative Closest Contour Point," *Intelligent Computation Technology and Automation, 2009. ICICTA '09. Second International Conference on* , vol.1, no., pp.245-249, 10-11 Oct. 2009

[15] Yi Lin; Lei Yan; Qingxi Tong; , "Underwater geomagnetic navigation based on ICP algorithm," *Robotics and Biomimetics, 2007. ROBIO 2007. IEEE International Conference on* , vol., no., pp.2115-2120, 15-18 Dec. 2007

[16] Leblond, I.; Legris, M.; Solaiman, B.; , "Use of classification and segmentation of sidescan sonar images for long term registration," *Oceans 2005 - Europe* , vol.1, no., pp. 322- 327 Vol. 1, 20-23 June 2005

[17] Zhiwen Zhu; Jiancheng Luo; Zhanfeng Shen; , "Automatic remote sensing image registration based on SIFT descriptor and image classification," *Geoinformatics, 2010 18th International Conference on* , vol., no., pp.1-5, 18-20 June 2010

[18] Chii-Jen Chen; , "3D Breast Tumor Classification Using Image Registration Framework," *Future Computer and Communication, 2009. ICFCC 2009. International Conference on* , vol., no., pp.153-157, 3-5 April 2009

[19] Yu-Ping Wang; , "M-FISH image registration and classification," *Biomedical Imaging: Nano to Macro, 2004. IEEE International Symposium on* , vol., no., pp. 57- 60 Vol. 1, 15-18 April 2004

[20] Kristy K. Brock; Laura A. Dawson; Michael B. Sharpe; Douglas J. Moseley; David A. Jaffray; , "Feasibility of a novel deformable image registration technique to facilitate classification, targeting, and monitoring of tumor and normal tissue, " *International Journal of Radiation Oncology*Biology*Physics*, Volume 64, Issue 4, 15 March 2006, Pages 1245-1254,

[21] Besl, P.J.; McKay, H.D.; , "A method for registration of 3-D shapes," *Pattern Analysis and Machine Intelligence, IEEE Transactions on* , vol.14, no.2, pp.239-256, Feb 1992

[22] Chen, Y.; Medioni, G.; , "Object modeling by registration of multiple range images," *Robotics and Automation, 1991. Proceedings., 1991 IEEE International Conference on* , vol., no., pp.2724-2729 vol.3, 9-11 Apr 1991

[23] Rusinkiewicz, S.; Levoy, M.; , "Efficient variants of the ICP algorithm," *3-D Digital Imaging and Modeling, 2001. Proceedings. Third International Conference on* , vol., no., pp.145-152, 2001

[24] Turk, G. and Levoy, M. "Zippered Polygon Meshes from Range Images," *Computer graphics and interactive techniques, 1994, Proceedings, 21st annual conference on*, 1994

[25] Masuda, T.; Sakaue, K.; Yokoya, N.; , "Registration and integration of multiple range images for 3-D model construction," *Pattern Recognition, 1996., Proceedings of the 13th International Conference on* , vol.1, no., pp.879-883 vol.1, 25-29 Aug 1996

[26] Weik, S.; , "Registration of 3-D partial surface models using luminance and depth information," *3-D Digital Imaging and Modeling, 1997. Proceedings., International Conference on Recent Advances in* , vol., no., pp.93-100, 12-15 May 1997

[27] Blais, G.; Levine, M.D.; , "Registering multiview range data to create 3D computer objects," *Pattern Analysis and Machine Intelligence, IEEE Transactions on* , vol.17, no.8, pp.820-824, Aug 1995

[28] Kari Pulli; Linda G. Shapiro; , "Surface Reconstruction and Display from Range and Color Data," *Graphical Models*, Volume 62, Issue 3, May 2000, Pages 165-201

[29] Pulli, K.; , "Multiview registration for large data sets," *3-D Digital Imaging and Modeling, 1999. Proceedings. Second International Conference on* , vol., no., pp.160-168, 1999

[30] Berthold K. P. Horn; Hugh M. Hilden; and Shahriar Negahdaripour; , "Closed-form solution of absolute orientation using orthonormal matrices," *J. Opt. Soc. Am.* A **5**, pp.1127-1135, 1988

[31] Michael W. Walker; Lejun Shao; Richard A. Volz; , "Estimating 3-D location parameters using dual number quaternions, " *CVGIP: Image Understanding*, Vol.54, pp 358-367, November 1991

[32] Daehwan Kim; Daijin Kim; , "A Fast ICP Algorithm for 3-D Human Body Motion Tracking," *Signal Processing Letters, IEEE* , vol.17, no.4, pp.402-405, April 2010

[33] Jost, T.; Hugli, H.; , "A multi-resolution scheme ICP algorithm for fast shape registration," *3D Data Processing Visualization and Transmission, 2002. Proceedings. First International Symposium on* , vol., no., pp. 540- 543, 2002

[34] Yan, P.; Bowyer, K.W.;, "A fast algorithm for ICP-based 3D shape biometrics," *Automatic Identification Advanced Technologies, 2005. Fourth IEEE Workshop on* , vol., no., pp. 213- 218, 17-18 Oct. 2005

[35] Yaser Sheikh; , "Image Registration, Source Code," *Internet:* www.cs.ucf.edu/~vision/source.html

[36] M. J. Procopio, "Hand-labeled DARPA LAGR datasets," *Internet:* http://www.mikeprocopio.com/labeledlagrdata.html ,2006-2007

[37] M. J. Procopio , "An Experimental Analysis of Classifier Ensembles for Learning Drifting Concepts Over Time in Autonomous Outdoor Robot Navigation," *PhD Thesis , University of Colorado at Boulder, USA*, 2007. Available at http://www.mikeprocopio.com/

[38] Duda, R. O. & P. E. Hart . *Pattern Classification and Scene Analysis*. New York: John Wiley & Sons, 1973

[39] Friedman Nir; Geiger Dan; Goldszmidt Moises; , "Bayesian Network Classifiers," *Machine Learning – Special issue on learning with probabilistic representations*, vol.29,pp 131-163, 1997

[40] John, G.; R. Kohavi; Pfleger K.; , "Irrelevant features and the subset selection problem," *Machine Learning: the Eleventh International Conference*, Proceedings of, pp.121-129, 1994

[41] Goldstein, M.;, " K_n-nearest neighbor classification," *Information Theory, IEEE Transactions on* , vol.18, no.5, pp. 627- 630, Sep 1972

[42] MacQueen, J;, "Some methods for classification and analysis of multivariate observations*," 5th Berkeley Symposium on Mathematical Statistics and Probability*, Proceesings of, University of California Press, pp.281–297, 1967

[43] James C Bezdek. *Pattern Recognition with Fuzzy Objective Function Algorithms*. Norwell, MA: Kluwer Academic Publishers, 1981

[44] Corinna Cortes and V. Vapnik. "Support-Vector Networks", Machine Learning, vol. 20, pp. 273-297,1995

[45] Pearson, K. *"On Lines and Planes of Closest Fit to Systems of Points in Space,*" Philosophical Magazine 2 (6),pp. 559–572, 1901